Quantum self-homodyne tomography with an empty cavity

Jing Zhang, Tiancai Zhang, Kuanshou Zhang, Changde Xie, and Kunchi Peng

Institute of Opto-Electronics, Shanxi University, Taiyuan 030006, China

Received November 29, 1999; revised manuscript received June 20, 2000

We develop a scheme to reconstruct the optical quantum state of a single-mode bright light field by using the dispersion characteristics of the empty cavity. The input field has a strong coherent component at frequency ω_0, which serves as a local oscillator (LO) to measure its two-sideband mode at $\omega_0 \pm \Omega$. We control the relative phase of the $0-2\pi$ range between the LO and the two-sideband mode by scanning the cavity length, so the optical quantum state is tomographically reconstructed. In the proposed scheme the influence of the space-mode mismatch between the LO and measured mode on the quantum efficiency is eliminated, and this scheme can conveniently be used in some quantum optical systems in which LO field cannot be available. © 2000 Optical Society of America [S0740-3224(00)01510-1]

OCIS code: 270.6570.

1. INTRODUCTION

There has been much interest in research in optical homodyne tomography in recent years. Significant advances in theory[1] and experiment[2–4] have been made. This kind of tomography allows one to reconstruct the Wigner function and the density matrix of a quantum state from a set of field quadratures measured by balanced homodyne detection. Reconstruction methods are based initially on an approximately inverse Radon transform of the quadrature histograms. To avoid a detour by means of the Wigner function and determine the density matrix directly from the measured quadrature distribution, algorithms for reconstructing the density matrix both from quadrature[5,6] and from photon number[7,8] have been developed. This method has proved to be stable and fast enough to permit real-time data sampling. The direct sampling approach to measuring the photon statistics of a semiconductor laser[9] and the density matrix of a squeezed vacuum has been implemented experimentally.[10] In optical homodyne tomography the set of distributions $\{P_\theta(x_\theta)\}$ is measured by optical homodyne detection, which is based on the interference between the signal field and a strong coherent reference field with an adjustable phase, that is, the local oscillator (LO); here $x_\theta = [\hat{a}\exp(-i\theta) + \hat{a}^+\exp(i\theta)]/\sqrt{2}$ is the phase-rotated quadrature amplitude. The quality of mode matching between the LO and the measured mode,[11] which is determined by their spatiotemporal overlap, directly influences the overall quantum efficiency of detection.[12] Moreover, it is difficult to use the LO beam in some practical systems, such as in the case of bright squeezed light from a frequency doubler and from a Kerr medium.

Recently a method of self-homodyne tomography[13] with which two-mode tomography can be performed from a twin-beam state at the output of a nondegenerate optical parametric amplifier was developed. One can also use self-homodyne tomography for two modes to measure the single-mode light from a degenerate optical amplifier. In the scheme proposed in Ref. 13, the strong mean field of a single mode at central frequency ω_0 was used as a LO to measure two-sideband mode $\omega_0 \pm \Omega$; here Ω is the analytic frequency for the reconstruction. The relative phase between the LO and the two-sideband mode was varied by scanning of the relative phase between the input signal field and the pump field. Thus homodyne tomography of the sidebands was accomplished.

In the research reported in Refs. 14–17 the phase of the squeezed state is controlled by a Fabry–Perot empty cavity; then the squeezing spectrum is measured. Here we develop the scheme of using a Fabry–Perot empty cavity to reconstruct the optical quantum state. The input field with a strong coherent component at frequency ω_0 serves as the LO with which to measure the two-sideband mode at $\omega_0 \pm \Omega$. According to the sidebands' frequency Ω, a suitable finesse of empty cavity is selected. One controls the relative phase between the LO and the two-sideband mode $\omega_0 \pm \Omega$ by scanning the cavity length; then the optical quantum state is tomographically reconstructed.

2. OPTICAL HOMODYNE TOMOGRAPHY OF A SINGLE MODE

Before introducing the tomography that uses an empty cavity, we briefly summarize the reconstruction of the Wigner function of a single-mode signal field described by photon annihilation and creation operators $\hat{a}$ and $\hat{a}^+$. Usually the reconstruction is accomplished by measurement of quadrature component distributions. As shown in Fig. 1, at a 50% beam splitter (B), signal wave ($\hat{a}$) spatially overlaps a strong coherent oscillator ($\hat{a}_{\mathrm{LO}}$) of the same frequency. The output light fields from the 50% beam splitter can be expressed in terms of input beams:

$$\hat{c}(t) = (\sqrt{2}/2)[\hat{a}(t) + \exp(i\theta)\hat{a}_{\mathrm{LO}}(t)],$$

$$\hat{d}(t) = (\sqrt{2}/2)[\hat{a}(t) - \exp(i\theta)\hat{a}_{\mathrm{LO}}(t)]. \qquad (1)$$

0740-3224/2000/111920-06$15.00

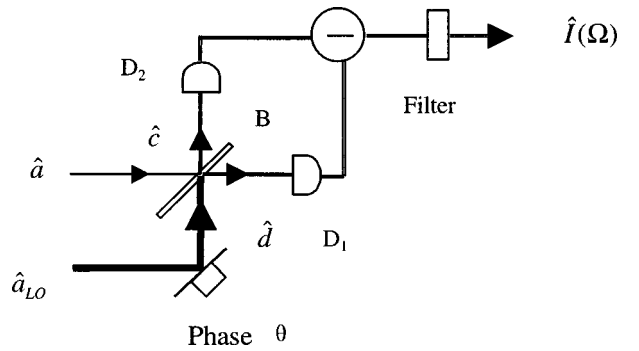

Fig. 1. Schematic of optical homodyne tomography.

Angle θ depends on the relative phase between the signal wave and the LO. The difference between photocurrents from detectors D1 and D2 placed at two output ports of the beam splitter is written as

$$\hat{I}_-(t) = \hat{c}^+(t)\hat{c}(t) - \hat{d}^+(t)\hat{d}(t) = \exp(i\theta)\hat{a}^+(t)\hat{a}_{\mathrm{LO}}(t) + \exp(-i\theta)\hat{a}^+_{\mathrm{LO}}(t)\hat{a}(t), \tag{2}$$

where $\hat{c}$, $\hat{c}^+$ and $\hat{d}$, $\hat{d}^+$ are the annihilation and creation operators, respectively, of the output light from the beam splitter. According to the semiclassical optical field method,[17] the fluctuating field can be considered a carrier $\hat{a}(\omega_0)$ oscillating at frequency ω_0 with an average value $\bar{a}(\omega_0)$ equal to that of the steady-state field a_{ss} which is surrounded by noise sidebands $\hat{a}(\omega_0 \pm \Omega)$ with zero average values

$$\bar{a}(\omega_0) = a_{ss}; \qquad \bar{a}(\omega_0 \pm \Omega \neq \omega_0) = 0. \tag{3}$$

A noise spectral component at frequency Ω can then be considered that of the hereodyne between the carrier and the noise sideband. For the usual experimental optical homodyne tomography systems the condition $\langle \hat{a}_{\mathrm{LO}} \rangle = \bar{a}_{\mathrm{LO}}(\omega_0) \gg \langle \hat{a} \rangle$ is always satisfied; then the output photocurrent at the analyzed frequency Ω is given as

$$\hat{I}_-(\Omega) = \bar{a}_{LO}(\omega_0)[\exp(-i\theta)\hat{a}(\omega_0 - \Omega) + \exp(i\theta)\hat{a}^+(\omega_0 + \Omega)]. \tag{4}$$

The quadrature component of the measured signal field is

$$\hat{X}(\theta, t) = [\hat{a}(t)\exp(-i\theta) + \hat{a}^+(t)\exp(i\theta)]/\sqrt{2}, \tag{5}$$

where $\hat{a}(t) = \hat{\alpha}(t)\exp(-i\omega_0 t)$ and $\hat{\alpha}(t)$ is the slowly varying electric field amplitude. $\hat{X}(\theta, t)$ is Fourier transformed into[18]

$$\hat{X}(\theta, \Omega) = [\hat{a}(\omega_0 - \Omega)\exp(-i\theta) + \hat{a}^+(\omega_0 + \Omega)\exp(i\theta)]/\sqrt{2}, \tag{6}$$

with

$$[\hat{a}(\omega_0 - \Omega), \hat{a}^+(\omega_0 - \Omega')] = 2\pi\delta(\Omega - \Omega'). \tag{7}$$

From Eqs. (4) and (6) it is obvious that the difference in the photocurrents is directly proportional to the quadrature component of the signal field. Thus, assuming that the signal field does not change during the measurement time, $\hat{I}_-(\Omega)$ furnishes an image of the time evolution of the signal field, which has different quantum fluctuations at different phase angles.

The recorded noise trace is divided into sections $[\theta, \theta + \Delta\theta]$, $\theta \in [0, 2\pi]$, in each of which the statistical distribution of fluctuations of $\hat{I}_-(\Omega)$, that is, the probability distribution $P_\theta(x_\theta)$ of eigenvalues x_θ of quadrature $\hat{X}_\theta$, is formed. These distributions are the projection integrals of Wigner function $W(x, y)$ of the signal state in rotating coordinates:

$$P_\theta(x_\theta) = \int_{-\infty}^{\infty} W(x_\theta \cos\theta - y_\theta \sin\theta, x_\theta \sin\theta + y_\theta \cos\theta)\mathrm{d}y_\theta, \tag{8}$$

where $y_\theta = -x\sin\theta + y\cos\theta$. The Wigner function is obtained from the set $\{P_\theta(x_\theta)\}$ by backprojection by use of the inverse Radon transform.[1] The alternative reconstruction method yields elements ρ_{nm} of the density matrix on a Fock basis by integration of $\{P_\theta\}$ over a set of pattern functions that were described in detail in Ref. 7. This method does not introduce any data filtering and in principle offers the possibility of on-line reconstruction, that is, of processing each data point directly after it is recorded.

3. THEORETICAL MODEL OF THE PROPOSED SCHEME

The proposed scheme for producing self-homodyne tomography of a single-mode field with an empty cavity is depicted in Fig. 2. In frequency space, the input single-mode field includes a strong coherent component $\hat{a}_0^{\mathrm{in}}(\omega_0)$ and a two-measured-sideband mode $\hat{a}_+^{\mathrm{in}}(\omega_0 + \Omega)$ and $\hat{a}_-^{\mathrm{in}}(\omega_0 - \Omega)$. In what follows, subscript 0 of $\hat{a}$ designates the center frequency ω_0 and subscript $\pm$ at the sidebands is $\omega_0 \pm \Omega$. ω_0 is typically an optical frequency, whereas Ω is a radio frequency. The input coupler is a partly reflecting mirror of amplitude-reflection coefficients r and transmission t ($r^2 + t^2 = 1$). Using the boundary conditions, we describe the field in the cavity by semiclassical method

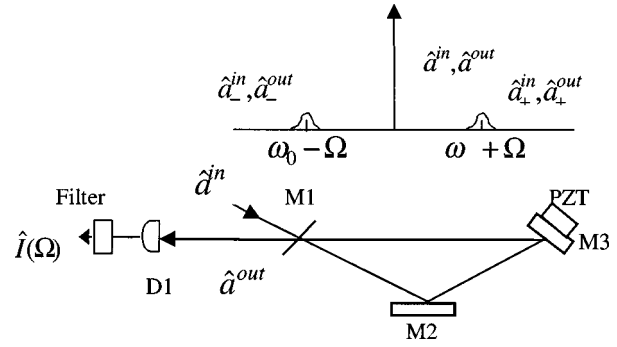

Fig. 2. Self-homodyne tomography with an empty cavity. The input field has a strongly coherent component at center frequency ω_0. The output field reflected by the empty cavity is directly detected, and a narrow band of the output photocurrents is selected, centered about frequency $\Omega \ll \omega_0$. PZT, piezoelectric transducer; M2, M3, high reflectors.

$$\hat{a}' = r\hat{a} + t\hat{a}^{\text{in}},$$
$$\hat{a}^{\text{out}} = t\hat{a} - r\hat{a}^{\text{in}},$$
$$\hat{a} = r_1\hat{a}' \exp(i\phi_0) + \sqrt{1 - r_1^2}\hat{a}_{\text{vac}}, \tag{9}$$

where $\hat{a}$ and $\hat{a}'$, respectively, are the intracavity fields just before and just after reflection by input–output coupler M1. $\hat{a}^{\text{in}}$ and $\hat{a}^{\text{out}}$ are the input and output amplitudes, respectively, ϕ_0 is the cavity round-trip propagation phase shift, $1 - r_1$ stands for the total cavity losses, $\hat{a}_{\text{vac}}$ is the vacuum noise introduced from intracavity losses ($\langle \hat{a}_{\text{vac}} \rangle = 0$). The relations between the input and the output fields for the central frequency and the two-sideband mode are obtained from Eq. (9):

$$\hat{a}_0^{\text{out}} = \frac{r_1 - r\exp(-i\phi_0)}{\exp(-i\phi_0) - rr_1}\hat{a}_0^{\text{in}}(\omega_0) + \frac{t\sqrt{1 - r_1^2}}{\exp(-i\phi_0) - rr_1}\hat{a}_{\text{vac}},$$
$$\hat{a}_+^{\text{out}} = \frac{r_1 - r\exp[-i(\phi_0 + \Omega L/c)]}{\exp[-i(\phi_0 + \Omega L/c)] - rr_1}\hat{a}_0^{\text{in}}(\omega_0 + \Omega) + \frac{t\sqrt{1 - r_1^2}}{\exp[-i(\phi_0 + \Omega L/c)] - rr_1}\hat{a}_{\text{vac}},$$
$$\hat{a}_-^{\text{out}} = \frac{r_1 - r\exp[-i(\phi_0 - \Omega L/c)]}{\exp[-i(\phi_0 - \Omega L/c)] - rr_1}\hat{a}_0^{\text{in}}(\omega_0 - \Omega) + \frac{t\sqrt{1 - r_1^2}}{\exp[-i(\phi_0 - \Omega L/c)] - rr_1}\hat{a}_{\text{vac}}, \tag{10}$$

where phase detuning $\phi_0 = \omega_0 L/c + \varphi_r - 2\pi N$ (N an integer), $2\pi N = \omega_0 L_{\text{res}}/c + \varphi_r$, L is the real round-trip length of the cavity, which is varied in the scanning process, L_{res} designates that, at resonance, φ_r is the total phase shift in three cavity mirrors, and c is the speed of light in vacuum.

A. Ideal Empty Cavity

For an ideal empty cavity and neglecting all losses, Eqs. (10) are reduced to the following expressions:

$$\hat{a}_0^{\text{out}} = \frac{1 - r\exp(-i\phi_0)}{\exp(-i\phi_0) - r}\hat{a}_0^{\text{in}}(\omega_0),$$
$$\hat{a}_+^{\text{out}} = \frac{1 - r\exp[-i(\phi_0 + \Omega L/c)]}{\exp[-i(\phi_0 + \Omega L/c)] - r}\hat{a}_0^{\text{in}}(\omega_0 + \Omega),$$
$$\hat{a}_-^{\text{out}} = \frac{1 - r\exp[-i(\phi_0 - \Omega L/c)]}{\exp[-i(\phi_0 - \Omega L/c)] - r}\hat{a}_0^{\text{in}}(\omega_0 - \Omega). \tag{11}$$

From Eqs. (11) we obtain

$$\left|\frac{1 - r\exp[-i\phi_0]}{\exp[-i\phi_0] - r}\right| = 1, \qquad \overline{\hat{a}_0^{\text{out}}} = \overline{\hat{a}_0^{\text{in}}(\omega_0)} = \text{const}.$$

The noise character of the reflected field is unchanged, and only a phase shift is added on the field. We define the phase-shift angle of the output field:

$$\theta(\phi_0) = \text{Arg}\left[\frac{1 - r\exp(-i\phi_0)}{\exp(-i\phi_0) - r}\right]. \tag{12}$$

The phase-shift angle as a function of detuning ϕ_0 is shown in Fig. 3. When $\theta = \pi - \delta(\delta \to 0)$, the corresponding detuning frequency is Ω_π. The full width of the cavity dispersion, defined as $2\Omega_\pi$, is a function of r.

The output field reflected by the empty cavity is detected directly by photodiode D1 (Fig. 1). The output photocurrents filtered by a narrow-band filter at Ω are given by the operators[13]

$$\hat{I}(\Omega) \propto \int_{-\infty}^{+\infty} dt \exp(i\Omega t) :|\hat{\epsilon}(t)|^2:$$
$$= \int_{-\infty}^{+\infty} d\omega \hat{\epsilon}^+(\omega + \Omega)\hat{\epsilon}(\omega), \tag{13}$$

where :: denote a general normal-ordering annihilation operator of the output field. The output field can also be measured by use of balanced detection. The quantum state of the optical field is reconstructed by means of the photocurrent of the output field directly detected by D1, which equals the sum of two photocurrents in balanced homodyne detection. The tomography of the coherent state, which usually serves as a standard with which one can judge whether the measured field is nonclassical, is produced from the difference of photocurrents.[17] Because the input field has a strong coherent component only at center frequency ω_0, relation (13) is simplified to

$$\hat{I}(\Omega) = \hat{a}_0^{\text{out}+}\hat{a}^{\text{out}} + \hat{a}_+^{\text{out}+}\hat{a}_0^{\text{out}}. \tag{14}$$

In the process of direct detection, highly excited central mode $\hat{a}_0$ beats with the $\omega_0 \pm \Omega$ sideband modes; thus it plays the role of a LO in normal homodyne and hereodyne detectors. In this case the direct detection is converted into self-homodyne detection and the output from the detector becomes the measured rescaled values of the output photocurrents in the case of a strong LO:

$$\hat{i}(\Omega) = \lim_{|\hat{a}_0^{\text{out}}| \to \infty} \frac{\text{Tr}_{\text{LO}}[\hat{I}(\Omega)\hat{\rho}_{\text{LO}}]}{\sqrt{2}|\hat{a}_0^{\text{out}}|}, \tag{15}$$

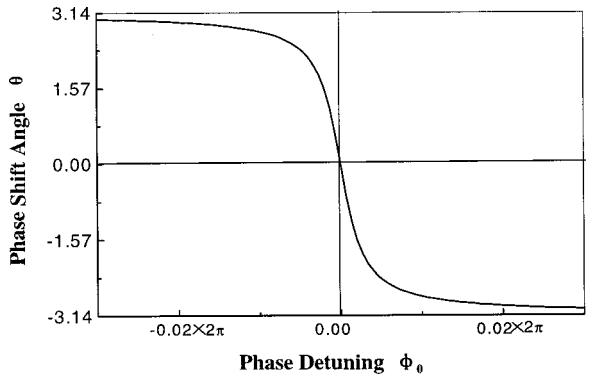

Fig. 3. Phase-shift angle as a function of phase detuning ϕ_0. $r = 0.9998$.

where $\hat{\rho}_{\mathrm{LO}}$ represents the density operator of the LO, $\mathrm{Tr}_{\mathrm{LO}}$ denotes the partial trace over the LO mode, and $|\hat{a}_0^{\mathrm{out}}|$ represents the average amplitude of the LO. Thus we obtain

$$\begin{aligned}\hat{i}(\Omega) &= \frac{1}{\sqrt{2}}\{\exp[i\theta(\phi_0)]\hat{a}_-^{\mathrm{out}} + \exp[-i\theta(\phi_0)]\hat{a}_+^{\mathrm{out}+}\} \\ &= \frac{1}{\sqrt{2}}\left(\exp\left\{i\left[\theta(\phi_0) - \theta\left(\phi_0 - \frac{\Omega L}{c}\right)\right]\right\}\hat{a}_-^{\mathrm{in}} \right. \\ &\quad \left. + \exp\left\{-i\left[\theta(\phi_0) - \theta\left(\phi_0 + \frac{\Omega L}{c}\right)\right]\right\}\hat{a}_+^{\mathrm{in}+}\right).\end{aligned} \tag{16}$$

As was shown in Ref. 1, reconstruction of the optical quantum state requires measurement of quadrature amplitude distributions of different phase angles by orthogonal phase-rotated transformation. The orthogonal phase-rotated transformation of an optical field can be reached by selection of the suitable full width $2\Omega_\pi$ of the empty cavity, which must be smaller than the measured sideband frequency Ω. By scanning the cavity length with a piezoelectric transduces, one can change the frequency detuning from $-\Omega_\pi$ to Ω_π. When $-(\Omega_\pi L/c) < \phi_0 < \Omega_\pi L/c$, from Eqs. (11) and (12) we obtain

$$\begin{aligned}&\theta\left(\phi_0 + \frac{\Omega L}{c}\right) \approx -\pi, \\ &\theta\left(\phi_0 - \frac{\Omega L}{c}\right) \approx \pi, \qquad \theta(\phi_0) \in [-\pi, \pi],\end{aligned} \tag{17}$$

and Eq. (16) is simplified to

$$\hat{i}(\Omega) = -(1/\sqrt{2})\{\exp[i\theta(\phi_0)]\hat{a}_-^{\mathrm{in}} + \exp[-i\theta(\phi_0)]\hat{a}_+^{\mathrm{in}+}\}. \tag{18}$$

Equation (18) gives the orthogonal phase-rotated transformation[1] when the phase-shift angle $\theta(\phi_0)$ is varied continuously from $-\pi$ to π. So the phase-shift range of 2π needed for tomography is gained [see approximations (17)]. Thus if we get a set of measured quadrature amplitude distributions for the different phase angles θ, we can construct the quantum state of the optical field by using an empty cavity. As an example, according to the calculation method described in Refs. 19 and 20, the variances of an amplitude-squeezed state at the various phase angles θ were calculated from a set of measured quadrature amplitude distributions and are shown in Fig. 4. The maximum squeezing was obtained at three detuning frequencies, which correspond to the phase-shift angles ($\theta = -\pi, 0, \pi$) of the orthogonal phase-rotated transformation. The sets of quadrature amplitude distributions between phase-shift angles from $\theta = -\pi$ to $\theta = \pi$ satisfy the condition of orthogonal phase-rotated transformation in approximation (17) and are used for quantum-state reconstruction. The data of the phase-shift angles outside $\theta \in [-\pi, \pi]$ are nonorthogonal phase-rotated transformations and are useless for reconstruction. The zero line of the ordinate in Fig. 4 is the level of the shot-noise limit.

B. Nonideal Empty Cavity

In the above calculations we assumed a perfect single-ended cavity without any losses. In fact, even on highly reflecting mirrors, losses from absorption, scattering, and transmission are inevitable. If r_1 expresses the total extra losses, the field reflected by the cavity is then given by Eqs. (10). From Eqs. (10) we obtain the average value of output field:

$$\overline{\hat{a}_0^{\mathrm{out}}} = \frac{r_1 - r\exp(-i\phi_0)}{\exp(-i\phi_0) - rr_1}\overline{\hat{a}_0^{\mathrm{in}}(\omega_0)}. \tag{19}$$

The amplitude and the phase shift of the output field are totally changed when detuning ϕ_0 is varied. We define the phase-shift angle of the output field:

$$\theta'(\phi_0) = \mathrm{Arg}\left[\frac{rr_1\exp(-i\phi_0) - 1}{r_1\exp(-i\phi_0) - r}\right]. \tag{20}$$

The phase-shift angle as a function of detuning ϕ_0 is shown in Fig. 4. When $\theta' = \pi - \delta(\delta \to 0)$, the corresponding frequency detuning is Ω'_π. So the full width of the cavity dispersion is defined as $2\Omega'_\pi$, which is a function of r and r'. It is obvious from Eqs. (10) that the full width of the empty cavity is wider than the ideal cavity, and the amplitude of output field is changed owing to the intracavity losses r_1, as shown in Fig. 5. For tomography we should also ensure that the measured sideband frequency $\Omega > 2\Omega'_\pi$. When the scanning frequency range is $-\Omega'_\pi$ to Ω'_π, Eqs. (10) are reduced to the following expressions:

$$\begin{aligned}\overline{\hat{a}_0^{\mathrm{out}}} &= \frac{r_1 - r\exp(-i\phi_0)}{\exp(-i\phi_0) - rr_1}\overline{\hat{a}_0^{\mathrm{in}}(\omega_0)} \\ &= \left|\frac{r_1 - r\exp(-i\phi_0)}{\exp(-i\phi_0) - rr_1}\right|\exp[i\theta'(\phi_0)]\overline{\hat{a}_0^{\mathrm{in}}(\omega_0)}, \\ &\quad \theta'(\phi_0) \in [-\pi, \pi], \quad \hat{a}_+^{\mathrm{out}} \approx -\hat{a}_0^{\mathrm{in}}(\omega_0 + \Omega), \\ &\quad \hat{a}_-^{\mathrm{out}} \approx -\hat{a}_0^{\mathrm{in}}(\omega_0 - \Omega).\end{aligned} \tag{21}$$

When the empty cavity is scanned, the coherent amplitude component at center frequency ω_0 is varied. As the coherent amplitude component is used as the strong LO that is needed for measurement, it should be kept at a

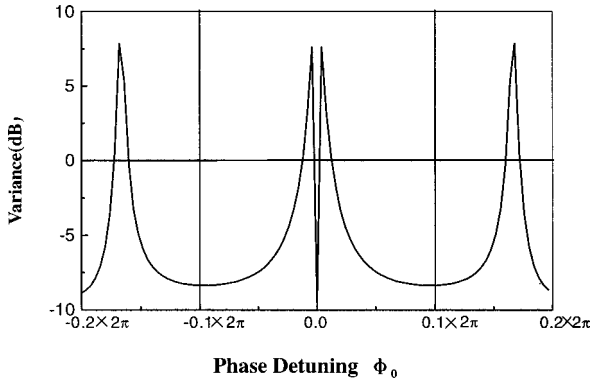

Fig. 4. Variance of the amplitude-squeezed coherent state numerically calculated relative to the detuning frequency of the scanned empty cavity at sideband mode frequency $2\pi\Omega = 500$ MHz. $L = 0.1$ m, $r = 0.9998$, and the amplitude squeezing is 90%.

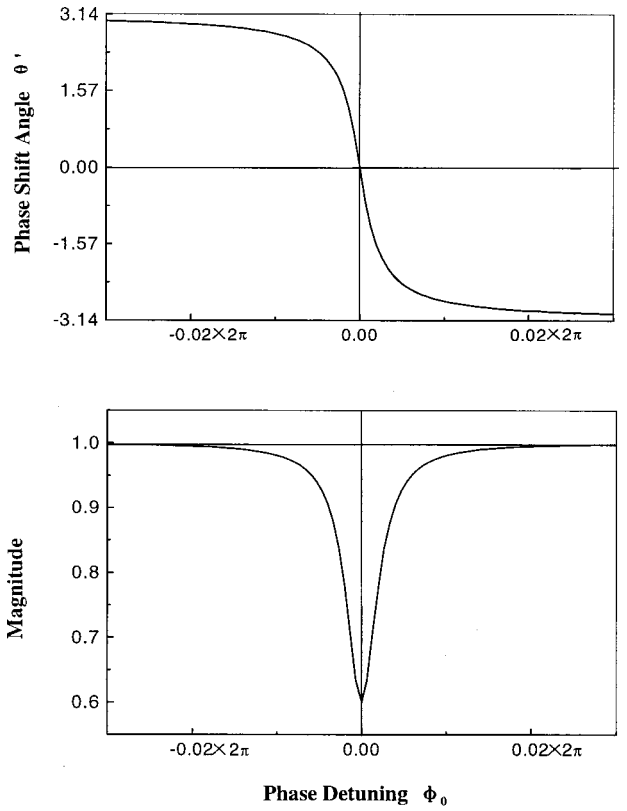

Fig. 5. Magnitude and phase of the reflected field relative to the input field for a nonideal empty cavity $r = 0.9998$.

specific intensity that is easy to reach by choice of the appropriate cavity parameters. The influence on the measured data that is due to variance of the LO intensity during cavity scanning can be eliminated through rescaling of Eq. (15). Expression (13) for the rescaled output photocurrents is simplified to

$$\hat{i}(\Omega) = -\frac{1}{\sqrt{2}}\{\exp[i\theta'(\phi_0)]\hat{a}_-^{\text{in}} + \exp[-i\theta'(\phi_0)]\hat{a}_+^{\text{in}+}\}. \tag{22}$$

Equation (22) is an orthogonal phase-rotated transformation when phase-shift angle $\theta'(\phi_0)$ is varied continually from $-\pi$ to π. The phase-shift range of 2π for tomography is also obtained. The sideband quantum character is not affected, because two sidebands are far from the resonant frequency and therefore all the sidebands are reflected without any loss. The measurement stability of the cavity length and the frequency of measured signal field should be sufficient to ensure the validity of measured data at different angles θ'.

4. CONCLUSIONS

In conclusion, we propose a self-homodyne detection scheme in which one uses the dispersion characteristics of an empty cavity to perform quantum tomography of a single mode that has a strong mean field. In the scheme, the influence of space-mode mismatch between the LO and the measured signal field on the quantum efficiency is eliminated, and this scheme can conveniently be used in some quantum-optical systems in which the LO field cannot be available. In this measurement scheme the analyzed frequency Ω must be larger than the full width of the empty cavity [see expressions (17)]; therefore, when the measurement is performed at a small analyzed frequency, a high-finesse cavity is required. In this case the requirement for stability of the cavity length and the signal frequency is correspondingly increased and is not easily met experimentally. However, the new self-homodyne tomography scheme is experimentally feasible for measurements in the range of larger analyzed frequencies.

ACKNOWLEDGMENTS

This research is supported by the National Natural Science Foundation of China (approval 69837010), the Excellent Young Teacher Foundation of the Education Department of China, and the Shanxi Province Science Foundation.

K. Peng's e-mail address is kcpeng@mail.sxu.edu.cn.

REFERENCES

1. K. Vogel and H. Risken, "Determination of quasiprobability distributions in terms of probability distributions for the rotated quadrature phase," Phys. Rev. A **40**, 2847–2849 (1989).
2. D. T. Smithey, M. Beck, M. G. Raymer, and A. Faridani, "Measurement of the Wigner distribution and the density matrix of a light mode using optical homodyne tomography application to squeezed states and the vacuum," Phys. Rev. Lett. **70**, 1244–1247 (1993).
3. D. T. Smithey, M. Beck, J. Cooper, and M. G. Raymer, "Measurement of number-phase uncertainty relations of optical fields," Phys. Rev. A **48**, 3159–3167 (1993).
4. G. Breitenbach, T. Muller, S. F. Pereira, J. Ph. Poizat, S. Schiller, and J. Mlynek, "Squeezed vacuum from a monolithic optical parametric oscillator," J. Opt. Soc. Am. B **12**, 2304–2309 (1995).
5. H. Kuhn, D. G. Welsch, and W. Vogel, "Determination of density matrices from field distributions and quasiprobilities," J. Mod. Opt. **41**, 1607–1613 (1994).
6. A. Zuchetti, W. Vogel, D. G. Welsch, and M. Tasche, "Direct sampling of density matrices in field-strength bases," Phys. Rev. A **54**, 1–4 (1996).
7. G. M. D'Ariano, C. Macchiavello, and M. G. A. Paris, "Detection of the density matrix through optical homodyne tomography without filtered back projection," Phys. Rev. A **50**, 4298–4302 (1994).
8. U. Leonhardt, M. Munroe, T. Kiss, T. Richter, and M. G. Raymer, "Sampling of the photon statistics and density matrix using homodyne detection," Opt. Commun. **127**, 144–160 (1996).
9. M. Munroe, D. Boggavarapu, M. E. Anderson, and M. G. Raymer, "Photon number statistics from the phase-averaged quadrature field distribution: theory and ultrafast measurement," Phys. Rev. A **52**, R924–R927 (1995).
10. S. Schiller, G. Breitenbach, S. F. Pereira, T. Muller, and J. Mlynek, "Quantum statistics of the squeezed vacuum by measurement of the density matrix in the number state representation," Phys. Rev. Lett. **77**, 2933–2936 (1996).
11. J. H. Shapiro and A. Shakeel, "Optimizing homodyne of detection of quadrature noise squeezing by local-oscillator selection," J. Opt. Soc. Am. B **14**, 232–239 (1997).
12. G. M. D'Ariano, U. Leonhardt, and H. Paul, "Homodyne detection of the density matrix of the radiation field," Phys. Rev. A **52**, R1801–R1804 (1995).

13. G. M. D'Ariano, M. Vasilyev, and P. Kumar, "Self-homodyne tomography of a twin-beam state," Phys. Rev. A **58**, 636–648 (1998).
14. R. M. Shelby, M. D. Levenson, S. H. Perlmutter, R. G. Devoe, and D. F. Walls, "Broad-band parametric deamplification of quantum noise in an optical fiber," Phys. Rev. Lett. **57**, 691–694 (1986).
15. P. Galatola, L. A. Lugiato, M. G. Porreca, P. Tombesi, and G. Leuchs, "System control by variation of the squeezing phase," Opt. Commun. **85**, 95–103 (1991).
16. Y. Qu, M. Xiao, G. S. Holliday, S. Singh, and H. J. Kimble, "Enhancement of photon antibunching by passive interferometry," Phys. Rev. A **45**, 4932–4943 (1992).
17. T. C. Zhang, J. P. Poizat, P. Grelu, J. F. Roch, P. Grangier, F. Marin, A. Bramati, V. Jost, M. D. Levenson, and E. Giacobino, "Quantum noise of free-running and externally-stabilized laser diodes," Quantum Semiclassic. Opt. **7**, 601–613 (1995).
18. C. Fabre and S. Reynaud, "Quantum noise in optical systems: a semiclassical approach," in *Fundamental Systems in Quantum Optics*, J. Dalibard, J. M. Raimond, and J. Zinn-Justin, eds. (Elsevier, Amsterdam, 1991), pp. 1–42.
19. G. Breitenbach, S. Schiller, and J. Mlynek, "Measurement of the quantum states of squeezed light," Nature **387**, 471–475 (1997).
20. G. Breitenbach and S. Schiller, "Homodyne tomography of classical and non-classical light," J. Mod. Opt. **44**, 2207–2225 (1997).